

Bi-cruciate stabilized total knee arthroplasty can reduce the risk of knee instability associated with posterior tibial slope

Masaru Hada ^{1,2}, MD, Hideki Mizu-uchi, MD, PhD ², Ken Okazaki, MD, PhD ³,

Takao Kaneko, MD, PhD ¹, Koji Murakami, MD ², Yuan Ma, MD ²,

Satoshi Hamai, MD, PhD ², Yasuharu Nakashima, MD, PhD ²

1: Department of Orthopaedic Surgery, Toho University School of Medicine, 2-17-6 Ohashi, Meguro-ku, Tokyo, 153-8515, Japan.

2: Department of Orthopaedic Surgery, Graduate School of Medical Sciences, Kyushu University, 3-1-1 Maidashi, Higashi-ku, Fukuoka, 812-8582, Japan.

3: Department of Orthopaedic Surgery, Tokyo Women's Medical University, 8-1 Kawada-cho, Shinjuku-ku, Tokyo, 162-8666, Japan.

Correspondence author: Hideki Mizu-uchi, MD, PhD
Department of Orthopaedic Surgery, Graduate School of Medical Sciences,
Kyushu University
3-1-1 Maidashi, Higashi-ku, Fukuoka city, Fukuoka, 812-8582, Japan
Tel: 81-92-642-5488 Fax: 81-92-642-5507
E-mail: himizu@ortho.med.kyushu-u.ac.jp

1 **Title**

2 Bi-cruciate stabilized total knee arthroplasty can reduce the risk of knee instability associated with

3 posterior tibial slope

4 **Abstract**

5 ***Purpose***

6 The purpose of this study was to evaluate the relationship between posterior tibial slope and knee
7 kinematics in bi-cruciate stabilized (BCS) total knee arthroplasty (TKA), which has not been
8 previously reported.

9 ***Methods***

10 This computer simulation study evaluated Journey 2 BCS components (Smith & Nephew, Inc.,
11 Memphis, TN, USA) implanted in a female patient to simulate weight-bearing stair climbing. Knee
12 kinematics, patellofemoral contact forces, and quadriceps forces during stair climbing (from 86°
13 to 6° of flexion) were computed in the simulation. Six different posterior tibial slope angles (0°
14 to 10°) were simulated to evaluate the effect of posterior tibial slope on knee kinematics and
15 forces.

16 ***Results***

17 At 65° of knee flexion, no anterior sliding of the tibial component occurred if the posterior tibial
18 slope was less than 10°. Anterior contact between the anterior aspect of the tibial post and the
19 femoral component was observed if the posterior tibial slope was 6° or more. An increase of 10°

20 in posterior tibial slope (relative to 0°) led to a 4.8% decrease in maximum patellofemoral contact
21 force and a 1.2% decrease in maximum quadriceps force.

22 ***Conclusion***

23 BCS TKA has a wide acceptable range of posterior tibial slope for avoiding knee instability if the
24 posterior tibial slope is less than 10°. Surgeons should prioritize avoiding adverse effects over
25 trying to achieve positive effects such as decreasing patellofemoral contact force and quadriceps
26 force by increasing posterior tibial slope. Our study helps surgeons determine the optimal
27 posterior tibial slope during surgery with BCS TKA; posterior tibial slope should not exceed 10°
28 in routine clinical practice.

29

30 **Keywords**

31 total knee arthroplasty, posterior tibial slope, knee instability, computer simulation, bi-cruciate
32 stabilized type

33

34 **Introduction**

35 Proper positioning of total knee arthroplasty (TKA) components is important for a good clinical
36 outcome. Compared with coronal and rotational alignments, sagittal alignment, especially the
37 acceptable range for posterior tibial slope, remains controversial [2,14]. Increased posterior tibial
38 slope can contribute to improved deep knee flexion [22] and reduce the quadriceps force required
39 for knee motion [20]. On the other hand, there are disadvantages such as posterior articular wear
40 of the insert [27] and knee instability, which can result in anterior tibial translation [9,19,21,28].
41 Although each of these advantages and disadvantages can be appreciated, the optimal range of
42 posterior tibial slope will also vary by implant design. Evaluating the effect of posterior tibial
43 slope on clinical results might be difficult because of the large variation in cutting errors [1]. In
44 addition, inter-individual differences in muscular strength and soft tissue conditions also can
45 obscure the effect of posterior tibial slope on patellofemoral contact forces and quadriceps forces.
46 A computer simulation model might be useful for evaluating the effect of posterior tibial slope on
47 several factors when other conditions remain constant.

48 Bi-cruciate stabilized (BCS) TKA was designed to overcome the disadvantage of
49 paradoxical motion of the femoral component with conventional posterior-stabilized (PS) TKA
50 [6]. The design concept behind BCS TKA is promoting normal knee kinematics by incorporating
51 both anterior and posterior post-cam mechanisms to replicate function of both the anterior cruciate

52 ligament (ACL) and posterior cruciate ligament (PCL). In addition, BCS TKA has asymmetrical
53 tibial articular geometry, which means a conforming medial compartment and a less conforming
54 lateral compartment in sagittal alignment. These features can stabilize the knee in the sagittal
55 alignment; several studies have reported that BCS TKA has in vivo kinematics that are closer to
56 those of the normal knee than conventional PS TKA [11,24]. However, the relationship between
57 posterior tibial slope and knee kinematics in BCS TKA has not been reported previously. In
58 addition, computer simulation can be used to measure patellofemoral contact forces and
59 quadriceps forces, which cannot be measured in vivo. It is useful for surgeons to appreciate
60 postoperative knee kinematics including instability, patellofemoral contact forces, and quadriceps
61 forces with varying posterior tibial slopes after BCS TKA. The purpose of this study was to
62 determine the acceptable range for posterior tibial slope with BCS TKA based on computer
63 simulation. The hypothesis is that BCS TKA has a more acceptable range of posterior tibial slopes
64 for avoiding knee instability based on the design concept and that it causes knee instability if the
65 posterior tibial slope is excessive, but is unlikely to cause knee instability when implanted using
66 regular surgical technique.

67

68 **Materials and Methods**

69 *Computer simulation*

70 This study evaluated the Journey 2 BCS components (Smith & Nephew, Inc., Memphis, TN, USA)
71 implanted in a female patient that is 162 cm in height and 58 kg in weight to simulate weight-
72 bearing stair climbing. All the components were implanted in an appropriate size (femoral
73 component: size 3, tibial component: size 3, insert: 9 mm, patella component: 29 mm). Initial
74 coordinates were determined using a computer-assisted design software program (Rhino; Robert
75 McNeel and Associates, Seattle, WA, USA) as reported in our previous studies [16,17,19].
76 The origin of the initial coordinates was the center of the asymmetrical tibial insert, which is the
77 intersection of the perpendicular bisector that made rectangles in both the anterior-posterior and
78 the medial-lateral dimensions. The most distal condylar points of the femoral component were set
79 on the surface of the tibial insert in the superior-inferior dimension.

80 The implant geometry was imported into a dynamic musculoskeletal modeling program
81 (LifeMOD/KneeSIM 2010; LifeModeler, Inc., San Clemente, CA, USA; Fig. 1). This model has
82 been reported as a useful tool for kinematic evaluation [15,19,23]. KneeSIM uses rigid body
83 dynamics to simulate weight-bearing stair climbing. The masses of the limb segments and body
84 weight generate a flexion moment on the knee, whereas the quadriceps muscle exerts an extension
85 moment. This musculoskeletal model of the knee included the medial collateral and lateral
86 collateral ligaments, quadriceps muscle and tendon, patellar tendon, and hamstring muscles. The

87 proximal attachment points of the medial collateral ligament and lateral collateral ligament were
88 defined as the most prominent epicondyles of the femur. Collateral ligaments were modeled as
89 nonlinear springs with material properties obtained from a published report [3]. Contact between
90 the tibiofemoral and patellofemoral articular surfaces was simulated. The hip and ankle joints had
91 all three rotational degrees of freedom. The ankle section had no translational degrees of freedom.
92 The hip section was constrained in the mediolateral and anteroposterior (AP) directions but was
93 free to translate vertically in the direction of gravity under axial forces that generate a flexion
94 moment at the knee.

95 ***Evaluation of knee kinematics and forces during computer simulation***

96 Knee kinematics, patellofemoral contact force, and quadriceps force were computed during stair
97 climbing (from 86° to 6° of knee flexion) in the simulation. For knee kinematics, AP translation
98 of the femoral component relative to the tibial insert and the lowest points of the medial and lateral
99 condyles on the surface of the tibial insert were evaluated. AP translation of the femoral
100 component relative to the tibial insert was defined as anterior (positive) or posterior (negative) to
101 the midline of the tibial tray.

102 Six different angles (0° to 10°) of posterior tibial slope were simulated to evaluate the
103 effect of posterior tibial slope on knee kinematics and forces in this study. A posterior tibial slope

104 of zero degrees was defined as perpendicular to the tibial mechanical axis, defined as the line
105 connecting the center of the insert to the center of the ankle. We changed the posterior tibial slope
106 angle at 2° intervals ranging from 0° to 10° based on the origin of the coordinates (the center of
107 the tibial insert) in the sagittal alignment.

108 The anterior post-cam mechanism in BCS TKA was also evaluated using a finite element
109 (FE) model when anterior contact between the anterior aspect of the tibial post and the femoral
110 component occurred with the knee near full extension. FE simulations were performed using
111 FEMAP (Siemens PLM Software, Plano, TX, USA). The femoral component, which is similar to
112 the Co-Cr-Mo alloy femoral component, was modeled as a linear elastic body. The tibial insert
113 consisting of ultra-high molecular weight polyethylene was modeled as a nonlinear elastoplastic
114 body. The Young's modulus was set at 220 GPa for the femoral component and 0.9 GPa for the
115 tibial insert. Poisson's ratio was set at 0.31 and 0.45, respectively. The mesh of the femoral
116 component and the tibial insert was generated based on 0.5 mm tetrahedral elements. The
117 generated mesh contained a total of 597,570; 637,093; and 493,919 nodes for the femoral
118 component and 500,530; 523,973; and 600,790 nodes for the tibial insert. The resulted from
119 having 405,722; 432,970; and 408,017 total elements for the femoral component and 346,627;
120 363,242; and 341,972 total elements for tibial insert, for simulations with posterior tibial slopes

121 of 6°, 8° and 10°, respectively. The maximum von Mises stress on the anterior aspect of the tibial
122 post was analyzed.

123 *Validation of the computer simulation model*

124 Clinical (in vivo) data were used to validate the computational model. Fifteen knees (3 male and
125 12 female) received the Journey 2 BCS implant used in our computer simulation. Seven of these
126 knees were chosen to validate the computer model after matching for sex and implant size
127 (femoral component: size 3, tibial component: size 3, insert: 9 mm, patella component: 29 mm).
128 Mean age was 71.9 ± 2.5 years, mean posterior tibial slope was $3.1^\circ \pm 1.8^\circ$, and mean
129 postoperative follow-up was 13.0 ± 1.8 months. Continuous sagittal radiographic images were
130 obtained in each patient during stair climbing using a flat-panel detector (Hitachi, Clavis, Tokyo,
131 Japan), and analyzed using a 2D-3D image-matching technique [8]. The lowest points of the
132 medial and lateral condyles relative to the tibial insert in the computer simulation were compared
133 to clinical data. This study was approved by the institutional review board of Kyushu University
134 (No. 25–74). Informed consent was obtained from all patients prior to study participation.

135 *Statistical analysis*

136 To investigate the reliability and reproducibility of measurement in this simulation, intraobserver
137 and interobserver reliabilities were assessed by intraclass correlation coefficients [ICC (1,1) and

138 ICC (2,1), respectively] [26]. All measurements were done by two orthopedic surgeons (MH and
139 YM) at an interval of more than 1 week. The ICC (1,1) and ICC (2,1) of the measurement in this
140 simulation were perfect.

141

142 **Results**

143 *Knee kinematics in the simulation*

144 The femoral components translated anteriorly during stair climbing (from 86° to 6° of flexion)
145 (Fig. 2). Increases in posterior tibial slope resulted in a more posterior position of the femoral
146 component relative to the tibial insert and reduced the amount of AP translation. At 65° of knee
147 flexion, anterior sliding of the tibial component occurred only when the posterior tibial slope was
148 10° (Fig. 2). At 65° of knee flexion, there was an area of contact between the posterior aspect of
149 the tibial post and the femoral component if the posterior tibial slope was less than 10°, but there
150 was no engagement of the post-cam system at 10° (Fig. 3).

151 Anterior contact between the anterior aspect of the tibial post and the femoral component
152 was observed with the knee near full extension if the posterior tibial slope was 6° or more (Fig.
153 2). In contrast, no anterior contact occurred when the posterior tibial slope was less than 6°, and
154 there was no contact between the anterior aspect of the tibial post and the femoral component.

155 ***Patellofemoral contact force and quadriceps force in the simulation***

156 Both patellofemoral contact force and quadriceps force increased rapidly at 65° of knee flexion
157 when maximum vertical load was placed on the knee joint (Fig. 4, 5). After peaking, the forces
158 decreased gradually with knee extension. Increasing posterior tibial slope decreased both types of
159 maximum forces at 65° of knee flexion (Table 1). An increase of 10° in posterior tibial slope
160 (relative to 0°) led to a 4.8% decrease in maximum patellofemoral contact force and a 1.2%
161 decrease in maximum quadriceps force.

162 ***Knee contact conditions in the simulation***

163 Figure 6 shows contours of equivalent maximum von Mises stress on the anterior aspect of the
164 tibial post when anterior contact occurred near full knee extension. The area of contact was a
165 horizontal band on the anterior aspect of the tibial post. Concentrated stress on the center of the
166 anterior aspect of tibial post was observed when the posterior tibial slope was above 6°. Maximum
167 equivalent von Mises stress increased by increasing posterior tibial slope.

168 ***Validation: comparing simulation and in vivo knee kinematics***

169 In the computer model, the lowest points of both the medial and lateral condyles in the femoral
170 component were similar to the measured in vivo data (Fig 7, 8). The lowest point on the medial
171 condyle of the femoral component was located almost in the center of tibial insert and the lowest

172 point of the lateral condyle had moved from a posterior position to the center during knee
173 extension. The predicted knee kinematics were almost within the range of inter-specimen
174 variability.

175

176 **Discussion**

177 The most important findings of the present study were that BCS TKA has a wide acceptable range
178 of posterior tibial slope that avoids knee instability, even though increased posterior tibial slope
179 can result in knee instability similar to anterior sliding of the tibial component. This study showed
180 that no anterior sliding of the tibial component occurs if the posterior tibial slope is less than 10°.
181 Kim et al. reported that many postoperative knees achieved postoperative sagittal alignment of
182 the tibial component between 0° to 7° [10]. Therefore, BCS TKA is unlikely to cause knee
183 instability when implanted using regular surgical techniques even though the computer simulation
184 showed that anterior sliding of the tibial component occurs with 10° of posterior tibial slope.

185 Increases in posterior tibial slope induce a more posterior position of the femoral
186 component. A more posterior contact position between the femorotibial components leads to a
187 greater quadriceps lever arm, which improves the efficiency of movement and contributes to
188 lower quadriceps and patellofemoral contact forces [7,25]. In the present study, increasing

189 posterior tibial slope decreased both maximum forces at 65° of knee flexion, but the rate of
190 decrease from 0° to 10° was relatively small (4.8% for maximum patellofemoral contact force
191 and 1.2% for maximum quadriceps force). In contrast, increasing posterior tibial slope results in
192 anterior sliding of the tibial component, which should be avoided for long-term TKA success
193 [5,13]. Hamai et al. reported that increasing posterior tibial slope was linked to anterior sliding of
194 the femoral component during mid-flexion of the knee using a 2D-3D image-matching technique
195 [9]. Surgeons should prioritize adverse effects over the positive effect of increasing posterior tibial
196 slope for long-term survival.

197 This study used KneeSIM as the modeling program; several papers have reported that it
198 yields reproducible simulations of knee kinematics [4,15,17,18]. From our simulated model
199 validated with in vivo data, the lowest points of both the medial and lateral condyle translated
200 anteriorly with BCS TKA. The amount of translation on the lateral side was greater than on the
201 medial side during stair climbing. Knee kinematics in the simulation showed similar trends and
202 was almost within the range of inter-specimen variability for the clinical in vivo data. BCS TKA
203 incorporates both anterior and posterior post-cam mechanisms to reduce abnormal kinematics
204 resulting from AP instability by replicating cruciate ligament function. In addition, the tibial
205 articular geometry with BCS TKA guides posterior motion during knee flexion with less posterior

206 motion in the medial compartment than the lateral compartment. Our simulation model showed
207 knee kinematics that were consistent with the design concept of BCS TKA.

208 A 15% decrease in maximum patellofemoral contact force and a 6% decrease in
209 maximum quadriceps force with a 15° increase in posterior tibial slope (relative to 0°) were shown
210 in our previous computer simulation study of conventional PS TKA [19]. Anterior sliding of the
211 tibial component at 65° of knee flexion occurred with more than 5° of posterior tibial slope and
212 anterior contact between the tibial post and the femoral component was observed near full
213 extension with more than 10° of posterior tibial slope. The knee kinematics of BCS TKA and
214 conventional PS TKA are different even through all the same parameters were used in both studies.

215 BCS TKA had a more acceptable range of posterior tibial slope than conventional PS
216 TKA with regards to anterior sliding of the tibial component at 65° of knee flexion. One of the
217 main reasons is the shape of the tibial insert, which was designed to be medially concave and
218 laterally convex in the sagittal plane. In addition, the posterior lip is higher than the anterior lip
219 on the medial side of the tibial insert. These features can result in a sustainable stable condition
220 during stair climbing by increasing posterior tibial slope. Our study suggested that BCS TKA has
221 an area of contact area between the posterior aspect of the tibial post and the femoral component
222 that prevents excessive posterior translation of the medial compartment if the posterior tibial slope
223 was less than 10°.

224 Anterior contact between the anterior aspect of the tibial post and the femoral component
225 occurred above 6° of posterior tibial slope with BCS TKA in this study. The BCS TKA anterior
226 post-cam mechanism is located more anteriorly than that of conventional PS TKA to replicate the
227 function of the ACL in a normal knee. Anterior contact between the tibial post and the femoral
228 component in PS TKA was observed near full extension with posterior tibial slope of 10° or more
229 in our previous computer simulation; however, this contact was unexpected because it was not
230 part of the design concept. In contrast, the results of BCS TKA were not surprising given the
231 design of the anterior post-cam mechanism. Kuwashima et al. reported that Journey 2 BCS
232 demonstrated no excessive peak stress at any flexion angle based on contact stress analysis of the
233 anterior tibial post because of the concave femoral anterior cam and convex aspect of the tibial
234 post in the axial plane [12]. They also reported that the percentage of contact area was lower than
235 with other PS designs. Anterior contact is considered relatively safe because our study also
236 suggested that contact stress was less with a smaller posterior tibial slope.

237 There are several limitations to this study. First, only weight-bearing stair climbing was
238 analyzed because we compared the computer simulation with the same activity that had available
239 clinical data and our previous study using conventional PS TKA. Second, only one model size
240 (small female knee) was simulated with BCS TKA in this study. The condition of the knee might
241 be more complicated with cruciate-retained TKA due to the effect of posterior tibial slope on PCL

242 function [21,28]. As the design concept for BCS TKA is to promote normal knee kinematics, it
243 may be affected more by posterior tibial slope differences than PS TKA. Finding from our model
244 cannot be generalized to the entire patient population. In addition, the soft tissue material
245 properties were not subject specific; instead, they were based on the literature. Tanaka et al.
246 suggested that more exact simulation results can be generated by making an individual model
247 with patient-specific ligament insertion points, and that it would be possible to simulate various
248 postoperative conditions accurately for individual patients [23]. However, our computer model
249 was validated adequately with in vivo data, which contains inter-specimen variability. In addition,
250 we evaluated the effect of posterior tibial slope with other factors held constant. Third, clinical
251 conditions of the knee (e.g., postoperative knee scores) affected by posterior tibial slope were not
252 evaluated in the present study because the postoperative course of patients with in vivo data was
253 as short as one year. More research on long-term survival is necessary. Despite these limitations,
254 our study demonstrated the relationship between posterior tibial slope and knee kinematics in
255 BCS TKA. It was found that BCS TKA is more stable and that it is not as affected by increases
256 in posterior tibial slope. Our study helps surgeons determine the optimal posterior tibial slope
257 during surgery with BCS TKA; posterior tibial slope should not exceed 10° in routine clinical
258 practice.

259

260 **Conclusion**

261 BCS TKA is not associated with anterior sliding of the tibial component if the posterior tibial
262 slope is less than 10°. Surgeons should prioritize avoiding adverse effects over attempting to
263 achieve positive effects from increasing posterior tibial slope, even if BCS TKA is unlikely to
264 cause knee instability when implanted using regular surgical techniques.

265

266 **Acknowledgments**

267 We would like to thank Y. Wang and H. Higaki, Faculty of Engineering, Kyusyu Sangyo
268 University, Fukuoka Japan, for help in analyzing the data.

269

270 **List of Abbreviations**

271 TKA: total knee arthroplasty, BCS: bi-cruciate stabilized, PS: posterior-stabilized, ACL: anterior
272 cruciate ligament, PCL: posterior cruciate ligaments, AP: anteroposterior, FE: finite element, 2D:
273 2-dimensional, 3D: 3-dimensional, ICC: intraclass correlation coefficients, PTS: posterior tibial
274 slope

275

276 **Competing Interests**

277 Hideki Mizu-uchi: Zimmer Biomet; Paid presenter or speaker. Ken Okazaki: Zimmer Biomet;

278 Paid presenter or speaker. Smith & Nephew; Paid presenter or speaker. Johnson & Johnson; Paid
279 presenter or speaker. Pfizer Inc.; Research support. Cyfuse Inc.; Research support.

280

281 **Authors' Contributions**

282 MH collected and analyzed the data and drafted the manuscript. HM conceived of the study,
283 participated in its design, collected and analyzed the data and coordination and helped to draft the
284 manuscript. HM is also the corresponding author. KO collected and analyzed the data, and assisted
285 in drafting the manuscript. TK, KM and YM collected and analyzed the data. SH assisted in
286 drafting the manuscript. YN gave final approval to the manuscript.

287 **【References】**

- 288 1. Barrett WP, Mason JB, Moskal JT, Dalury DF, Oliashirazi A, Fisher DA (2011) Comparison
289 of radiographic alignment of imageless computer-assisted surgery vs conventional
290 instrumentation in primary total knee arthroplasty. *J Arthroplasty* 26(8):1273-1284
- 291 2. Barrack RL, Schrader T, Bertot AJ, Wolfe MW, Myers L (2001) Component rotation and
292 anterior knee pain after total knee arthroplasty. *Clin Orthop Relat Res.* 392:46-55
- 293 3. Blankevoort L, Kuiper JH, Huiskes R, Grootenboer HJ Articular contact in a three-
294 dimensional (1991) Articular contact in a three-dimensional model of the knee. *J Biomech*
295 24(11):1019-1031
- 296 4. Colwell CW Jr, Chen PC, D'Lima D (2011) Extensor malalignment arising from femoral
297 component malrotation in knee arthroplasty: effect of rotating-bearing. *Clin Biomech (Bristol,*
298 *Avon)* 26(1):52-57
- 299 5. Dejour D, Saffarini M, Demey G, Baverel L (2015) Tibial slope correction combined with
300 second revision ACL produce a good knee stability and prevents graft rupture. *Knee Surg*
301 *Sports Traumatol Arthrosc* 23:2846-2852
- 302 6. Dennis DA, Komistek RD, Mahfouz MR (2003) In vivo fluoroscopic analysis of fixed-
303 bearing total knee replacements. *Clin Orthop Relat Res* 410:114-30
- 304 7. D'Lima DD, Poole C, Chadha H, Hermida JC, Mahar A, Colwell CW Jr (2001) Quadriceps
305 moment arm and quadriceps forces after total knee arthroplasty. *Clin Orthop Relat Res*
306 392:213–220
- 307 8. Hamai S, Miura H, Higaki H, Matsuda S, Shimoto T, Sasaki K, Yoshizumi M, Okazaki K,
308 Tsukamoto N, Iwamoto Y (2008) Kinematic analysis of kneeling in cruciate-retaining and
309 posterior-stabilized total knee arthroplasties. *J Orthop Res* 26(4):435-442
- 310 9. Hamai S, Okazaki K, Shimoto T, Nakahara H, Higaki H, Iwamoto Y (2015) Continuous
311 sagittal radiological evaluation of stair-climbing in cruciate-retaining and posterior-stabilized
312 total knee arthroplasties using image-matching techniques. *J Arthroplasty* 30(5):864-869
- 313 10. Kim YH, Park JW, Kim JS, Park SD (2014) The relationship between the survival of total
314 knee arthroplasty and postoperative coronal, sagittal and rotational alignment of knee
315 prosthesis. *Int Orthop* 38:379–385
- 316 11. Kuroyanagi Y, Mu S, Hamai S, Robb WJ, Banks SA (2012) In vivo knee kinematics during
317 stair and deep flexion activities in patients with bicruciate substituting total knee arthroplasty.
318 *J Arthroplasty* 27(1):122–128
- 319 12. Kuwashima U, Hamai S, Okazaki K, Ikebe S, Higaki H, Mizu-Uchi H, Akasaki Y, Murakami
320 K, Iwamoto Y (2016) Contact stress analysis of the anterior tibial post in bi-cruciate stabilized
321 and mobile-bearing posterior stabilized total knee arthroplasty designs. *J Mech Behav*

- 322 Biomed Mater 60:460-467
- 323 13. Li G, Papannagari R, Most E, Park SE, Johnson T, Tanamal L, Rubash HE (2005) Anterior
324 tibial post impingement in a posterior stabilized total knee arthroplasty. *J Orthop Res*
325 23(3):536-541
- 326 14. Matsuda S, Kawahara S, Okazaki K, Tashiro Y, Iwamoto Y (2013) Postoperative alignment
327 and ROM affect patient satisfaction after TKA. *Clin Orthop Relat Res* 471(1):127-133
- 328 15. Mihalko WM, Conner DJ, Benner R, Williams JL (2012) How does TKA kinematics vary
329 with transverse plane alignment changes in a contemporary implant? *Clin Orthop Relat Res*
330 470(1):186-192
- 331 16. Mizu-uchi H, Colwell CW Jr, Matsuda S, Flores-Hernandez C, Iwamoto Y, D'Lima DD
332 (2011) Effect of total knee arthroplasty implant position on flexion angle before implant-bone
333 impingement. *J Arthroplasty* 26(5):721-727
- 334 17. Mizu-Uchi H, Colwell CW Jr, Fukagawa S, Matsuda S, Iwamoto Y, D'Lima DD (2012) The
335 importance of bony impingement in restricting flexion after total knee arthroplasty: computer
336 simulation model with clinical correlation. *J Arthroplasty* 27(9):1710-1716
- 337 18. Morra EA, Heim CS, Greenwald AS (2012) Preclinical computational models: predictors of
338 tibial insert damage patterns in total knee arthroplasty: AAOS exhibit selection. *J Bone Surg*
339 *Am* 94(18): e137(1-5)
- 340 19. Okamoto S, Mizu-uchi H, Okazaki K, Hamai S, Nakahara H, Iwamoto Y (2015) Effect of
341 tibial posterior slope on knee kinematics, quadriceps force, and patellofemoral contact force
342 after posterior-stabilized total knee arthroplasty. *J Arthroplasty* 30(8):1439-1943
- 343 20. Ostermeier S, Hurschler C, Windhagen H, Stukenborg-Colsman C (2006) In vitro
344 investigation of the influence of tibial slope on quadriceps extension force after total knee
345 arthroplasty. *Knee Surg Sports Traumatol Arthrosc* 14(10):934-939
- 346 21. Sessa P, Fioravanti G, Giannicola G, Cinotti G (2015) The risk of sacrificing the PCL in
347 cruciate retaining total knee arthroplasty and the relationship to the sagittal inclination of the
348 tibial plateau. *Knee* 22:51-55
- 349 22. Shi X, Shen B, Kang P, Yang J, Zhou Z, Pei F (2013) The effect of posterior tibial slope on
350 knee flexion in posterior-stabilized total knee arthroplasty. *Knee Surg Sports Traumatol*
351 *Arthrosc* 21(12):2696-2703
- 352 23. Tanaka Y, Nakamura S, Kuriyama S, Ito H, Furu M, Komistek RD, Matsuda S (2016) How
353 exactly can computer simulation predict the kinematics and contact status after TKA?
354 Examination in individualized models. *Clin Biomech (Bristol, Avon)* 39:65-70
- 355 24. Victor J, Mueller JK, Komistek RD, Sharma A, Nadaud MC, Bellemans J (2010) In vivo
356 kinematics after a cruciate- substituting TKA. *Clin Orthop Relat Res* 468(3):807-814
- 357 25. Wachowski MM, Walde TA, Balcarek P, Schüttrumpf JP, Frosch S, Stauffenberg C, Frosch

- 358 KH, Fiedler C, Fanghänel J, Kubein-Meesenburg D, Nägerl H (2012) Total knee replacement
359 with natural rollback. *Ann Anat* 194(2):195-199
- 360 26. Walter SD, Eliasziw M, Donner A (1998) Sample size and optimal designs for reliability
361 studies. *Stat Med* 17(1):101-110
- 362 27. Wasielewski RC, Galante JO, Leighty RM, Natarajan RN, Rosenberg AG (1994) Wear
363 patterns on retrieved polyethylene tibial inserts and their relationship to technical
364 considerations during total knee arthroplasty. *Clin Orthop Relat Res* 299:31-43
- 365 28. Zeng C, Yang T, Wu S, Gao SG, Li H, Deng ZH, Zhang Y, Lei GH (2016) Is posterior tibial
366 slope associated with noncontact anterior cruciate ligament injury. *Knee Surg Sports
367 Traumatol Arthrosc* 24:830-837

368 **Figure legends**

369 Fig. 1:

370 Lateral view of the LifeMOD/KneeSIM 2010 knee simulator model used in the present study

371 Fig. 2:

372 AP translation of the femoral component relative to the tibial insert during stair climbing

373 AP: anteroposterior

374 PTS: posterior tibial slope

375 Fig. 3:

376 Posterior contact of the BCS TKA post-cam at 65° of knee flexion (posterior view)

377 BCS: bi-cruciate stabilized

378 TKA: total knee arthroplasty

379 Fig. 4:

380 Patellofemoral contact force from 86° to 6° of knee flexion during simulated stair climbing

381 PTS: posterior tibial slope

382 Fig. 5:

383 Quadriceps force from 86° to 6° of knee flexion during simulated stair climbing

384 PTS: posterior tibial slope

385 Fig. 6:

386 Maximum equivalent stress distribution in the tibial insert with anterior contact (anterior view)

387 (a) Posterior tibial slope of 6°

388 (b) Posterior tibial slope of 8°

389 (c) Posterior tibial slope of 10°

390 Fig. 7:

391 Lowest point on the condyle of the femoral component relative to the tibial insert during stair
392 climbing from 70° to 10° of knee flexion based on simulated and in vivo data

393 (a) Lowest point on the medial condyle

394 (b) Lowest point on the lateral condyle

395 AP: anteroposterior

396 Fig. 8:

397 Lowest point on the condyle plotted on the tibial insert during stair climbing from 70° to 10° of
398 knee flexion

399 (a) Simulated data (posterior tibial slope of 4°)

400 (b) In vivo data (posterior tibial slope of 4.6°)

401

402

Figure 1

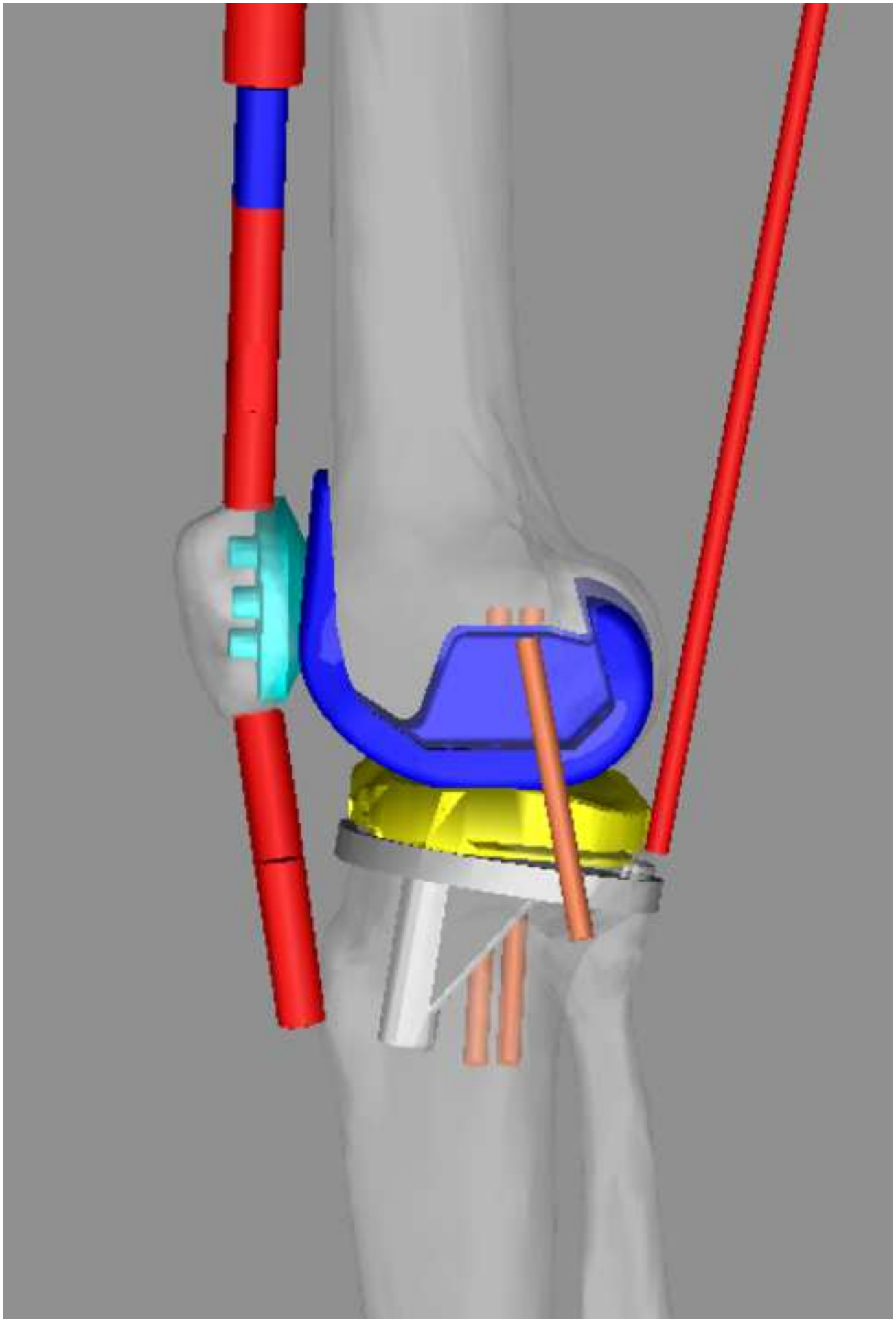


Figure 2

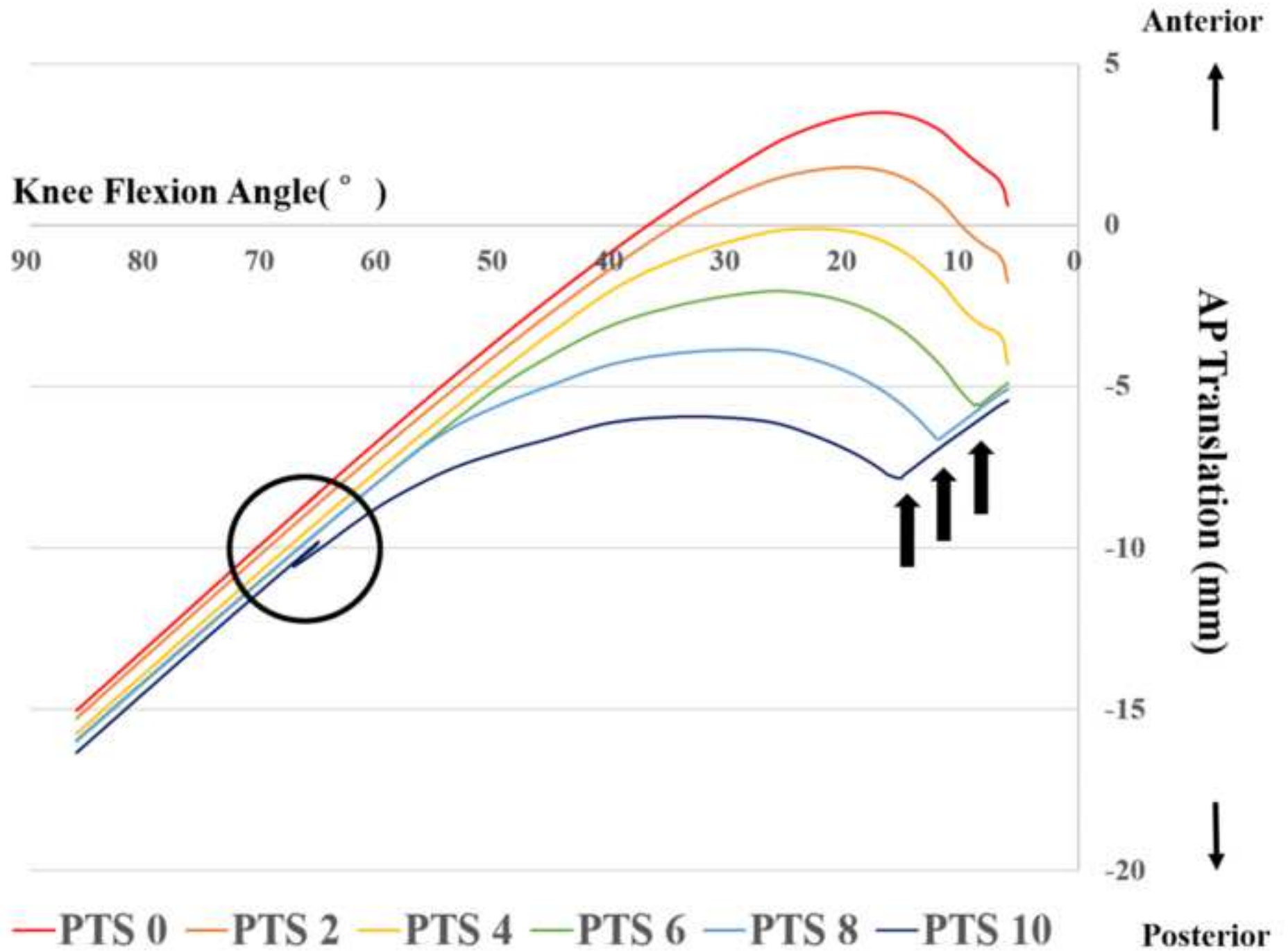


Figure 3

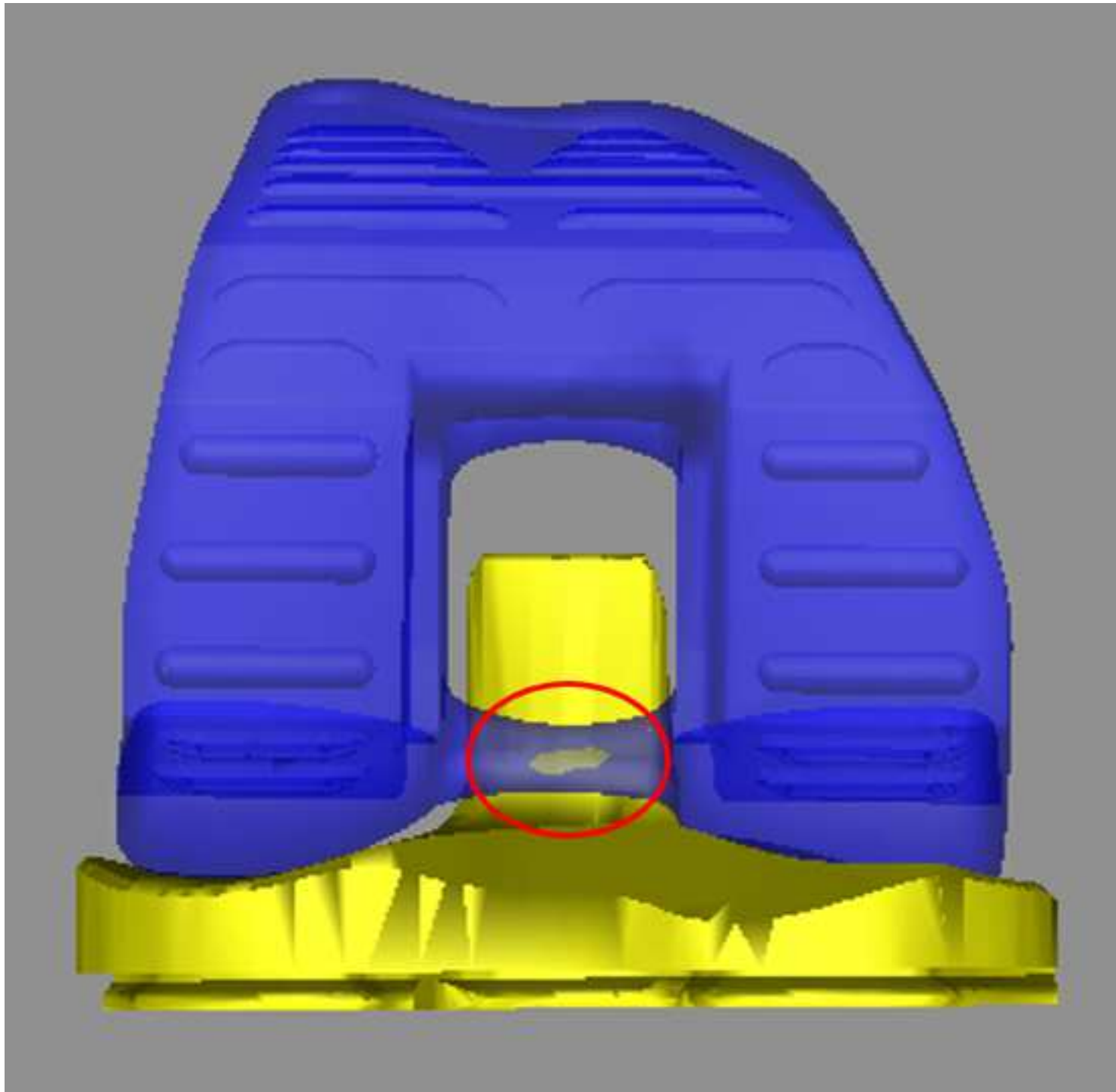


Figure 4

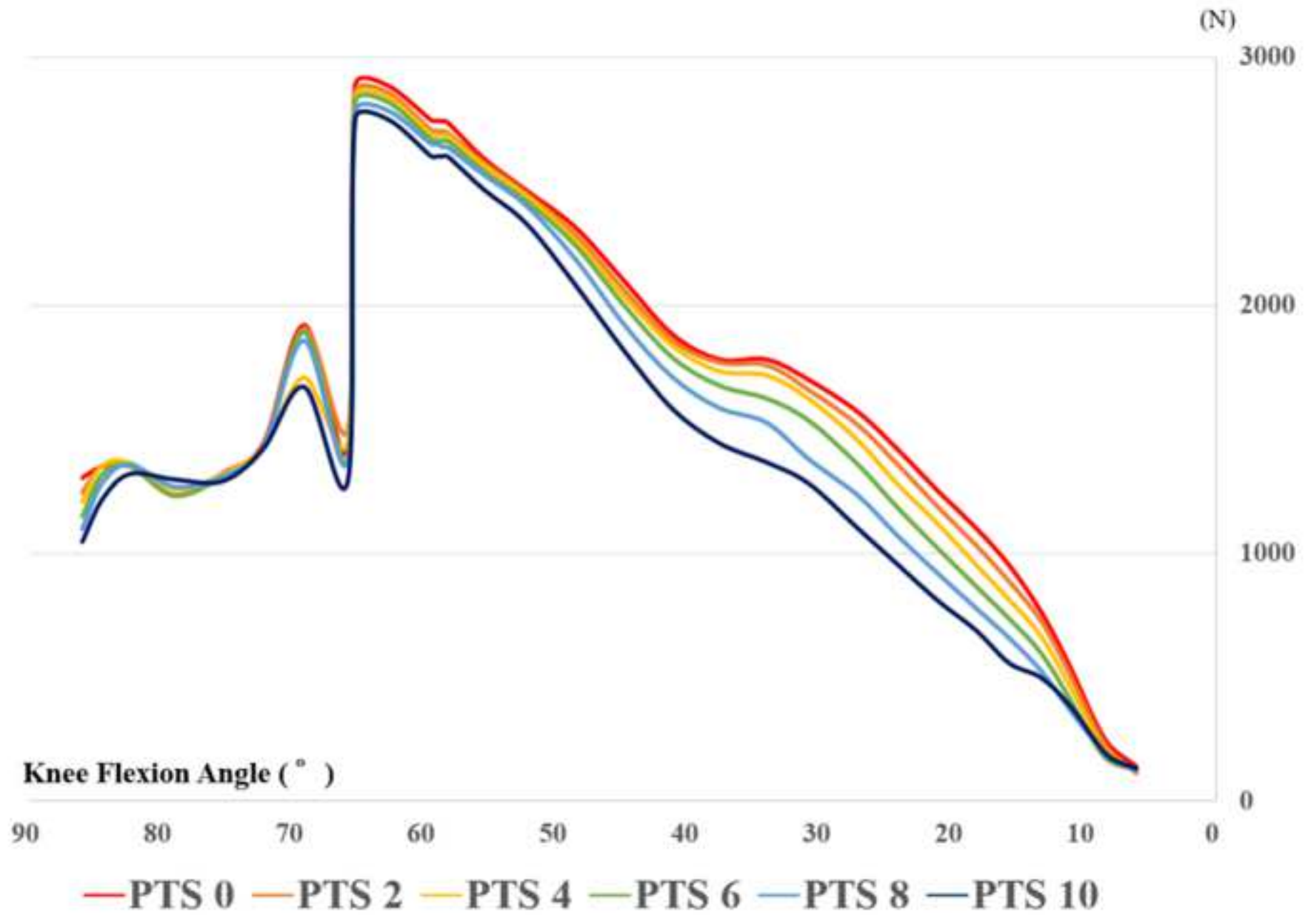


Figure 5

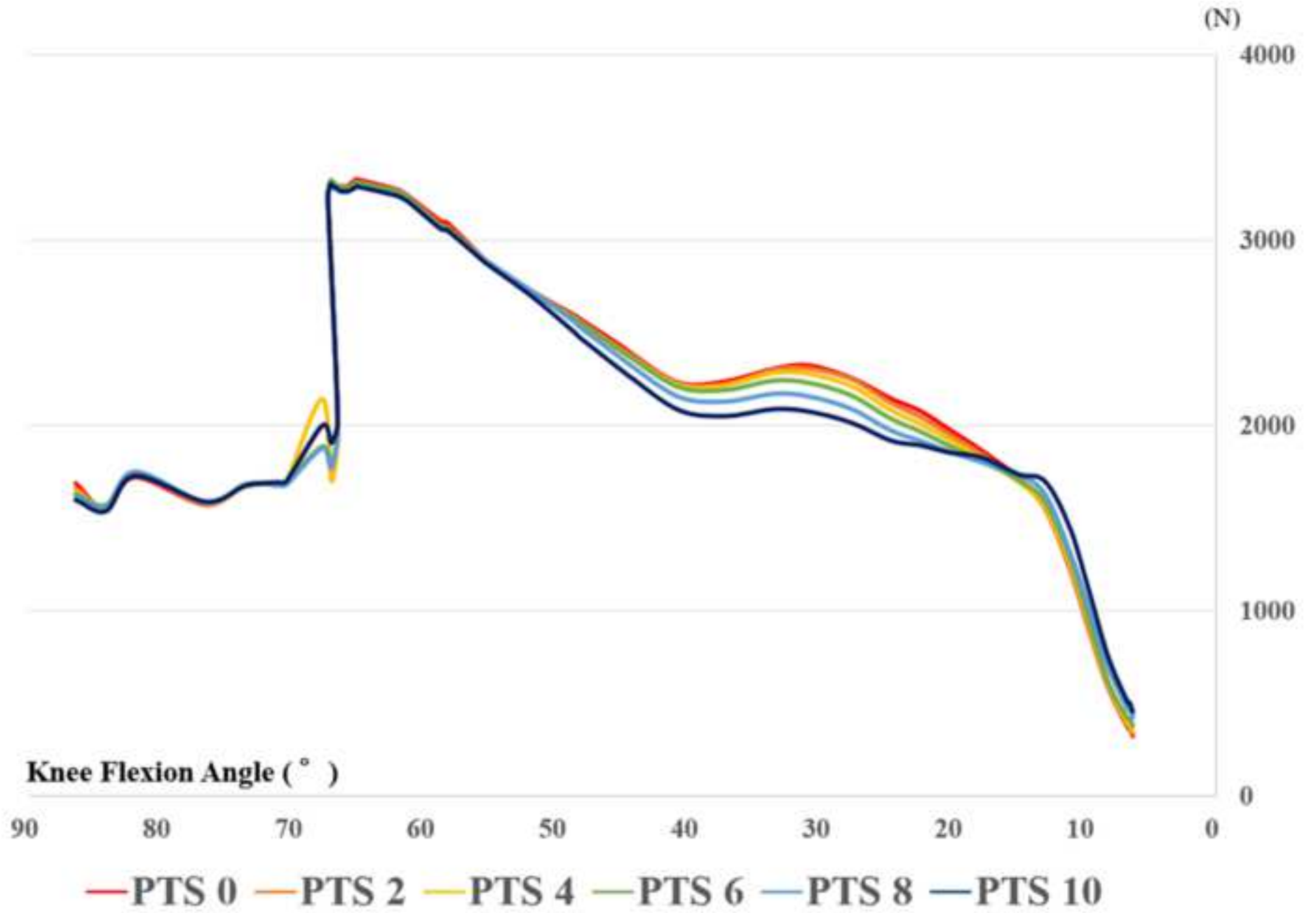


Figure 6

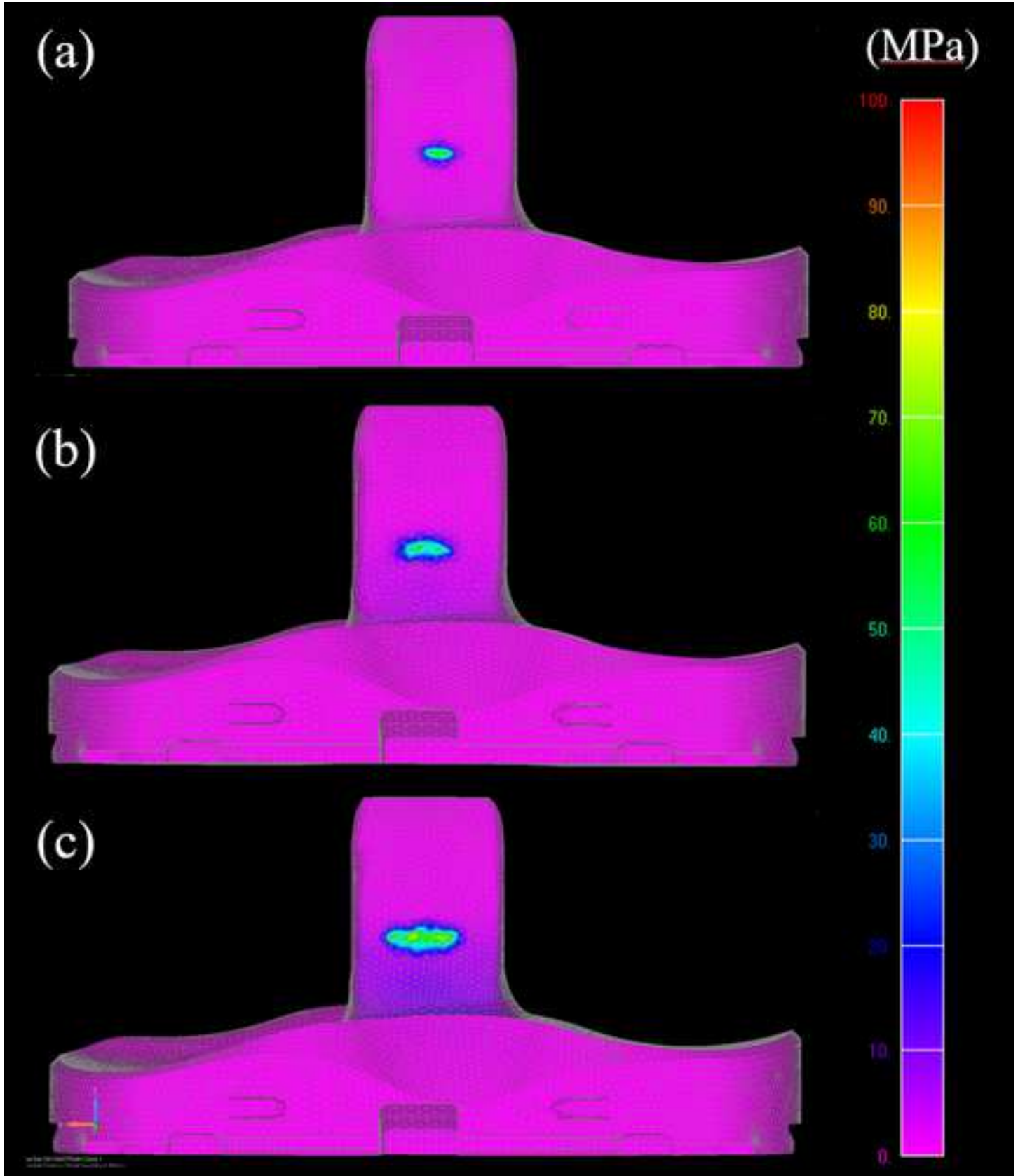
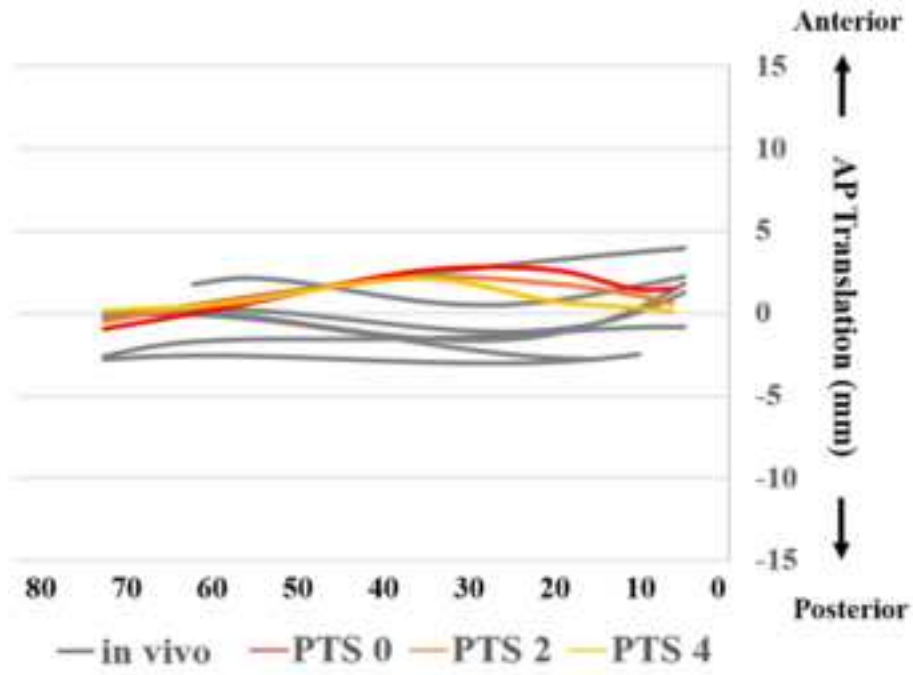
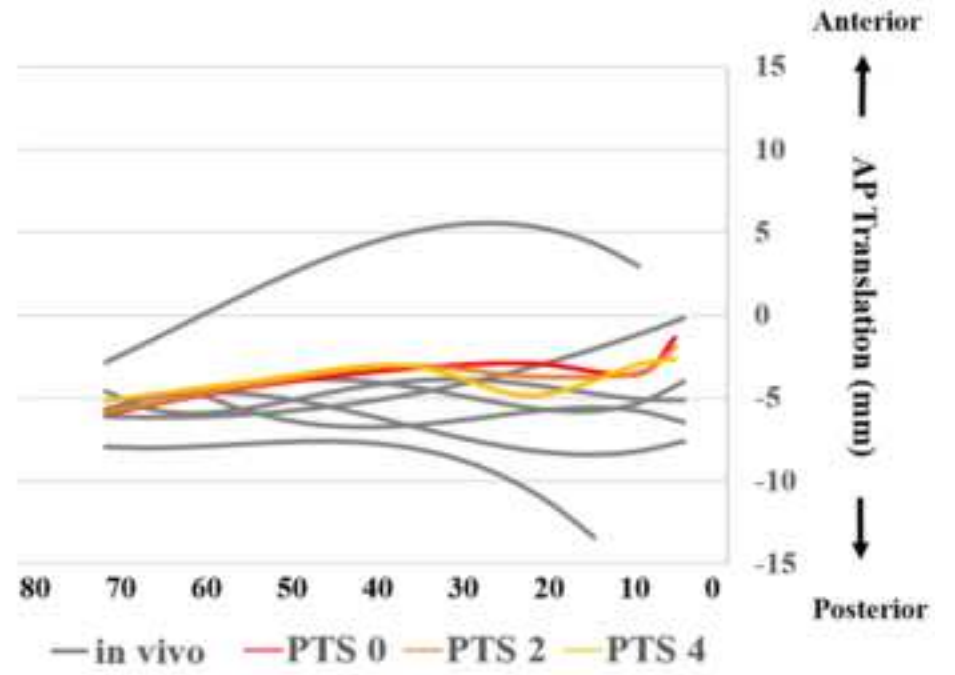


Figure 7



(a)



(b)

Figure 8

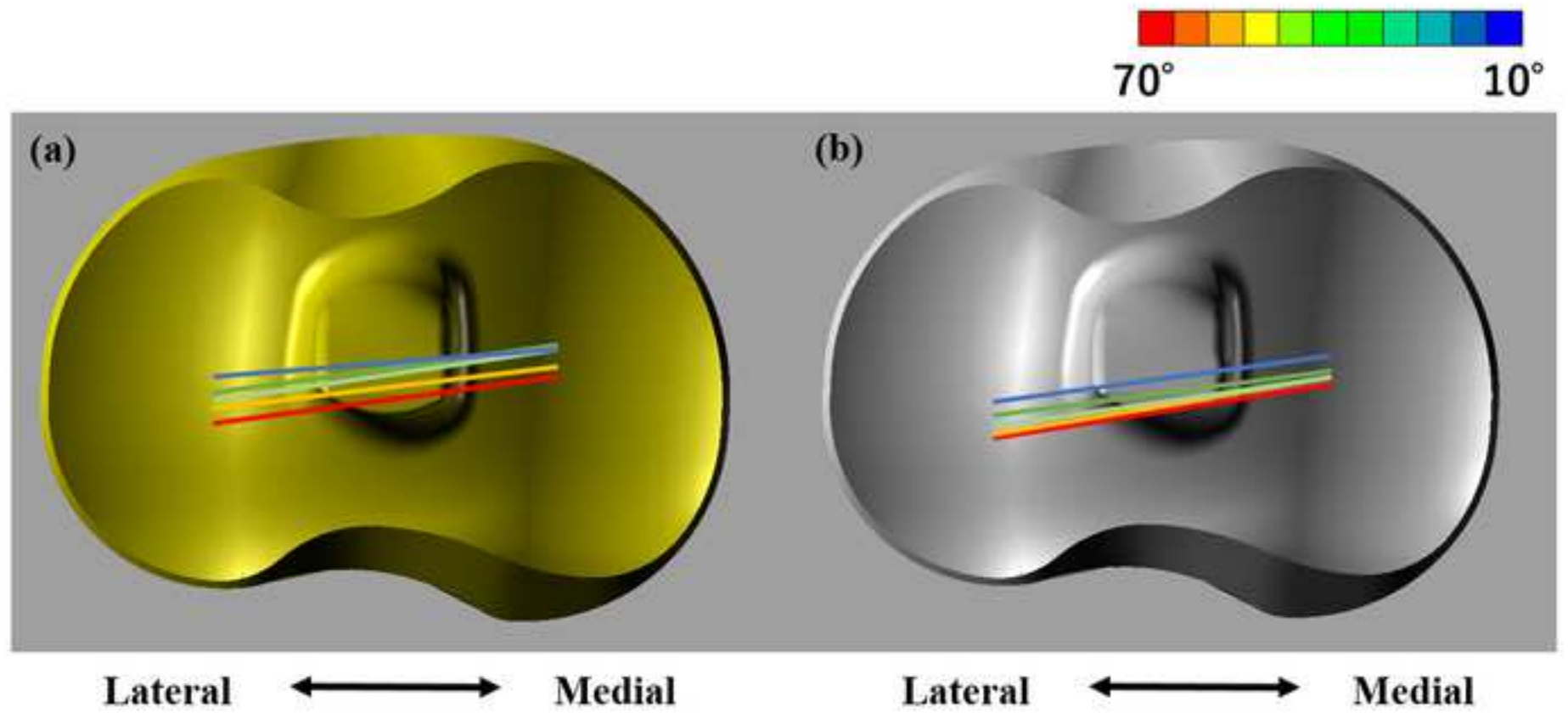


Table 1

Maximum patellofemoral contact force and quadriceps force at 65° of knee flexion in the simulation

Force	Posterior tibial slope					
	0°	2°	4°	6°	8°	10°
PF contact (N)	2935.8	2903.7	2882.9	2865.6	2826.3	2793.9
Quadriceps (N)	3369.2	3354.4	3350.8	3342.5	3330.5	3328.8

PF: patellofemoral